

## Supplementary information

### Probe Oscillation Control in Tapping-mode Scanning Probe Electro spray Ionization for Stabilization of Mass Spectrometry Imaging

Mengze Sun <sup>a</sup>, Yoichi Otsuka <sup>\*a,b</sup>, Maki Okada <sup>a</sup>, Shuichi Shimma <sup>c</sup> and Michisato Toyoda <sup>a,b</sup>

<sup>a</sup> Department of Physics, Graduate School of Science, Osaka University, Japan

<sup>b</sup> Forefront Research Center, Graduate School of Science, Osaka University, Japan

<sup>c</sup> Department of Bioengineering, Graduate School of Engineering, Osaka University, Japan

#### Contents:

Fig. S1 Calibration of piezo Z-stage using a laser displacement sensor. ....	2
Fig. S2 Comparison of data acquired for the A/P-D curve.....	3
Fig. S3 Flowchart of the algorithm used to read and separate the datasets. ....	4
Fig. S4 Data conversion to obtain A/P-D curves.....	5
Fig. S5 Detection of tapping point using second-order differentiated data of the oscillation phase. ....	6
Fig. S6 A/P-D curves with error bars. ....	7
Fig. S7 A/P-D curve measurements using the quartz substrate.....	8
Table S1 Parameter settings for the laser puller. ....	9

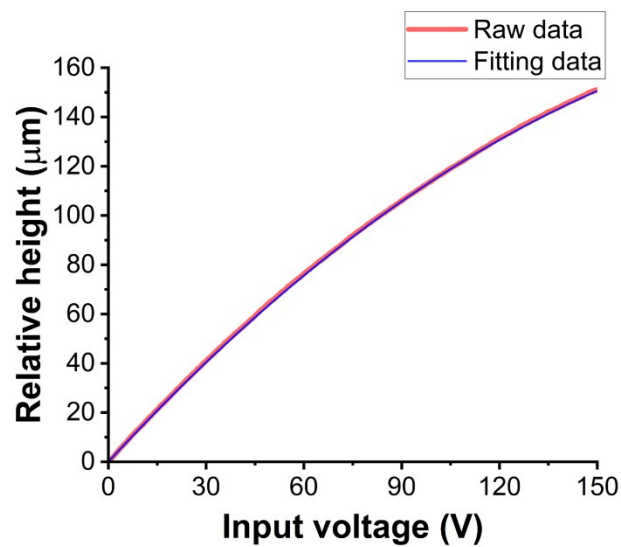


Fig. S1 Calibration of piezo Z-stage using a laser displacement sensor.

The height of the quartz substrate fixed on the piezo Z-stage was measured using a laser displacement sensor (CDX-L15, OPTeX FA Co., Ltd., Japan). The sample height was changed by inputting a triangular wave voltage from 0 to 150 V. The figure shows the relationship between the input voltage and relative height of the sample curves. The data were fitted with a polynomial function, which was used to calculate the sample height and obtain the A/P-D curves.

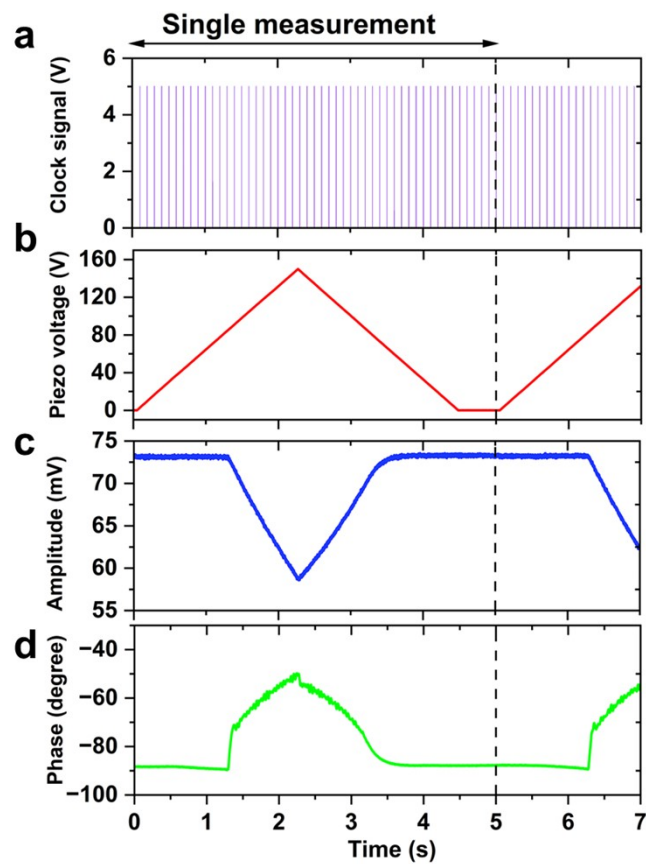
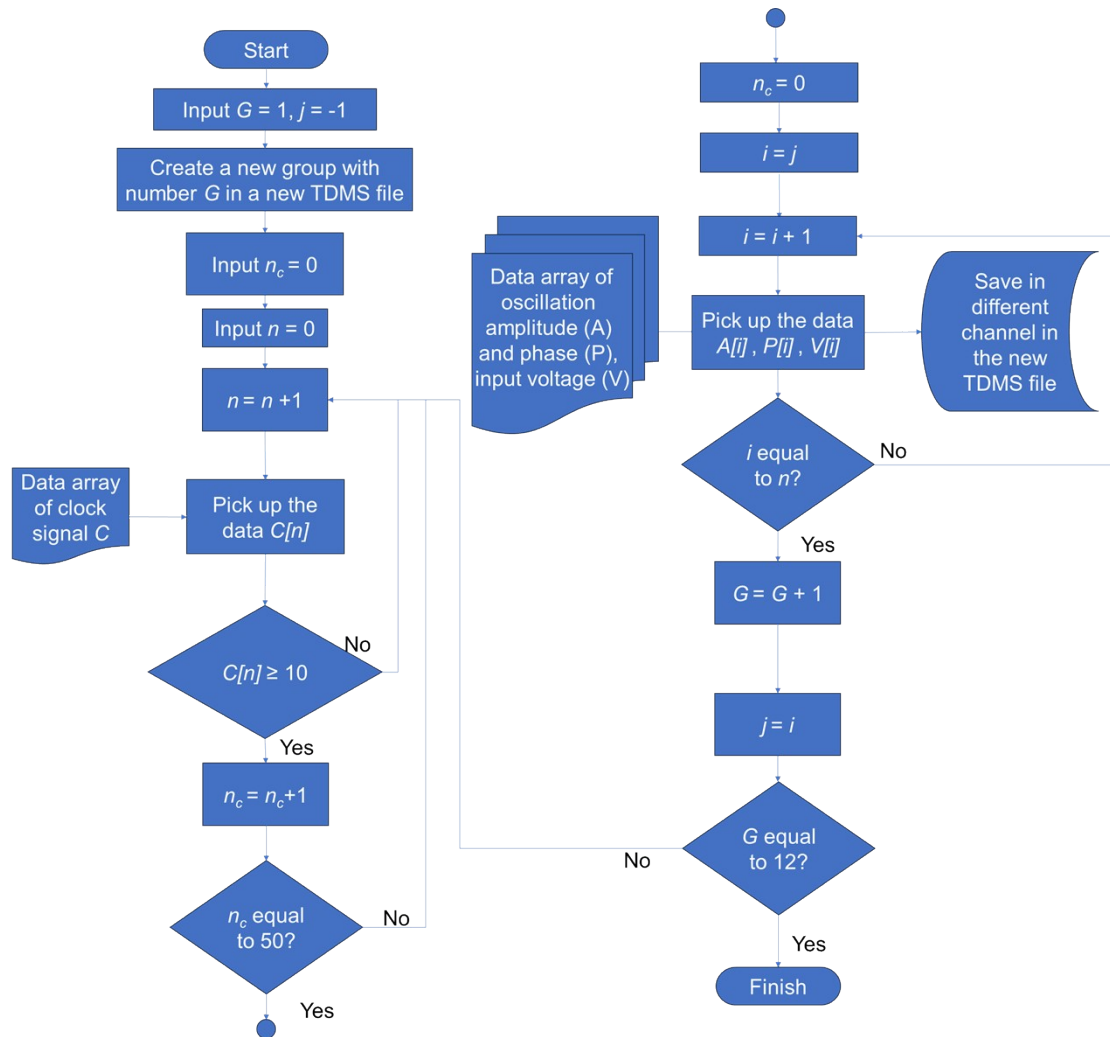


Fig. S2 Comparison of data acquired for the A/P-D curve.

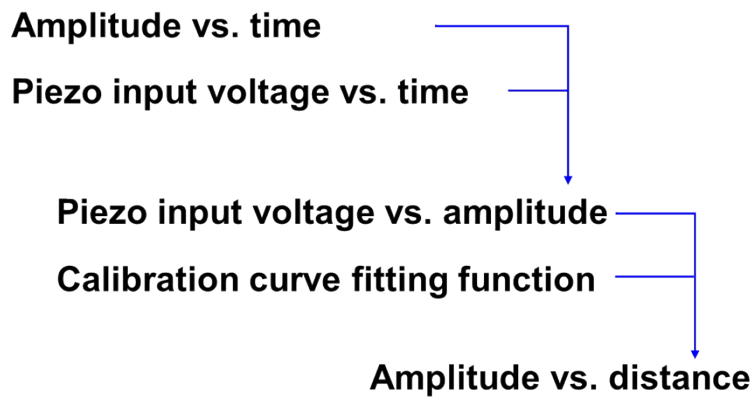
To control the timing of the sample stage movements, a square-wave voltage signal of 10 Hz was used as the clock signal (a). A triangular wave voltage signal (b) was used to control the height of the piezo Z-stage. The change in amplitude (c) and phase (d) were recorded simultaneously during the measurement. The total time for each measurement was 5 s.

Fig. S3 Flowchart of the algorithm used to read and separate the datasets.



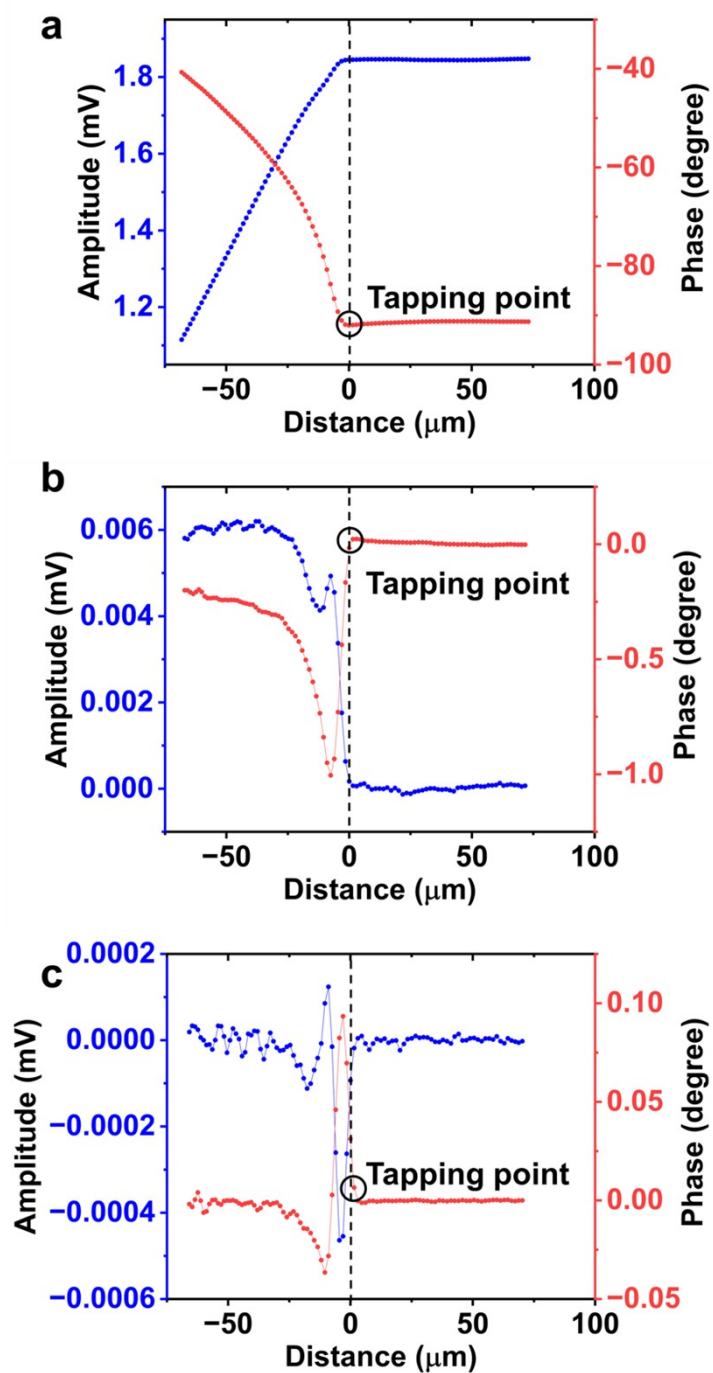
First, the group number  $G$  and data register  $j$ , a counter for the number of clock signals,  $n_o$ , and a counter for the number of data points,  $n$ , are initialized.  $G$  is the group number for different data, and register  $j$  is used to save the starting number of each group. A new group with a size of  $G$  is created in a new file (technical data management streaming (TDMS) format). Counter  $n$  indicates the number of data points that should be stored in group  $G$ . In the first loop, the data array of the clock signal is analysed. Because the clock signals are 0 V (OFF state) and 10 V (ON state), the transition of the clock signal is detected, and counter  $n_c$  is increased to 50. Next, counter  $n_c$  is reset, where  $n_c$  is counting how many data have been saved into each group, input counter  $i$ , and assign the value of  $j$  to  $i$ . The loop then selects other data, such as the oscillation amplitude from another array in another channel, and stores it in the new TDMS file. After selecting all the data points for this group, group number  $G$  is increased and the data number is saved to register  $j$ . Register  $j$  records the number of data points selected. For the next group, the data reading progress starts from here. This process is complete after all data are separated into 12 groups.

Fig. S4 Data conversion to obtain A/P-D curves.



The process of obtaining the amplitude vs. distance curve is shown. First, the relationships between the amplitude and time and between the piezo input voltage and time were selected. Next, these two datasets were merged to obtain the relationship between the piezo input voltage and amplitude. The calibration curve (Fig. S2) was used to convert the piezo input voltage into the relative height of the sample. Finally, the relationship between the oscillation amplitude and the distance between the tip and sample was obtained.

Fig. S5 Detection of tapping point using second-order differentiated data of the oscillation

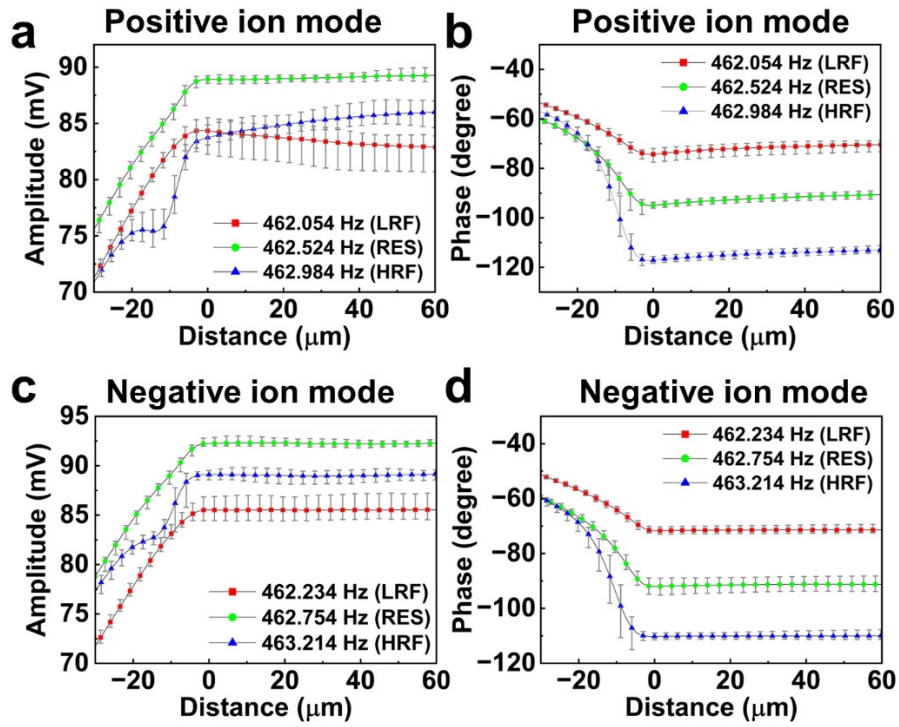


phase.

The figure shows the raw data (a), first-order differentiated data (b), and second-order differentiated data (c) for the A/P-D curve. The central finite-difference method was used in this calculation. The tapping point was located using the second-order differentiated data. The changes in amplitude and phase were much smaller, and setting a threshold of 0.001 for the phase curve effectively detected the jumping of the signal once the data exceeded the threshold. The tapping

point was defined by the jumping point in the second-order differentiated data of the phase vs. distance curve (red curve).

Fig. S6 A/P-D curves with error bars.



(a) and (b) show the A/P-D curve with error bar for the positive ion mode. (c) and (d) for the negative ion mode.



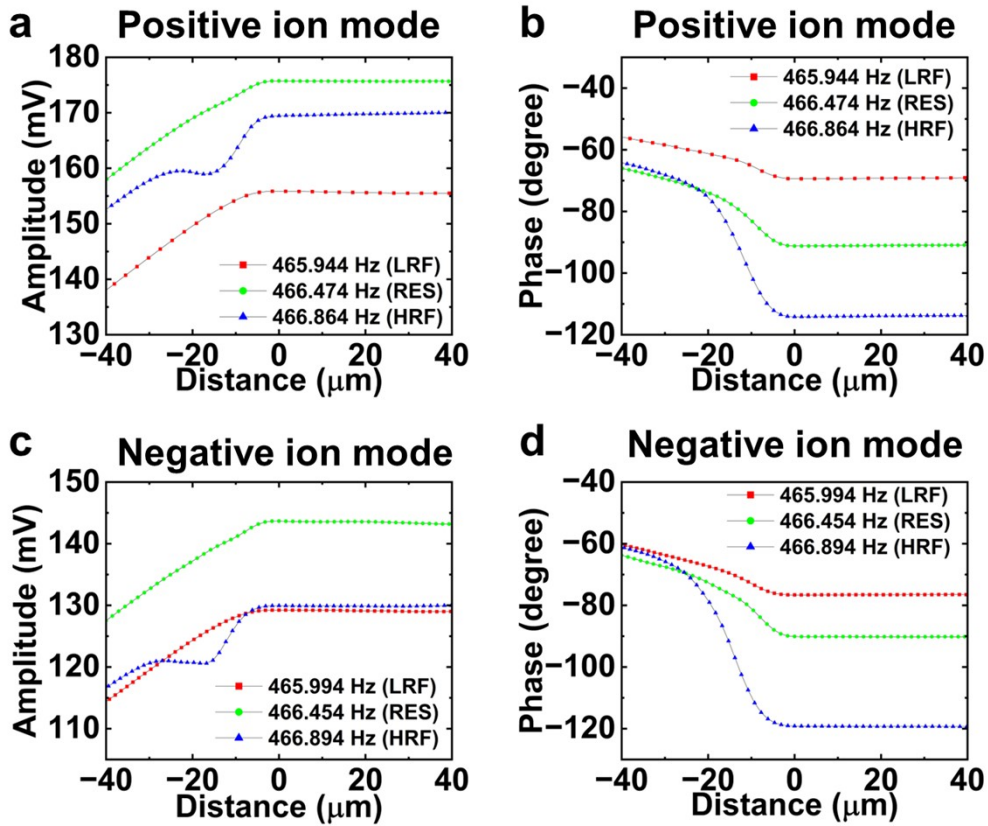


Fig. S7 A/P-D curve measurements using the quartz substrate.

The figure shows the A/P-D curve measurement on quartz. The initial distance between the probe tip and the sample surface was set at  $80\ \mu\text{m}$ . The applied voltage was set at  $2.5\ \text{kV}$  for positive ion mode and at  $-2.5\ \text{kV}$  for negative ion mode. The oscillation frequency was set at approximately  $465\ \text{Hz}$ . The phase values were adjusted to  $-70^\circ$ ,  $-90^\circ$ , and  $-110^\circ$  for the LRF, RES, and HRF, respectively. In positive ion mode, the oscillation amplitude (a) and phase (b) were also kept unchanged before the probe tapping of the sample surface. This means that a net attractive interaction was not generated for the quartz. After the probe tapped the quartz (distance  $< 0$ ), the amplitude decreased, and the nonlinear region was obtained for the HRF condition. The oscillation phase increased due to the repulsive interaction of three oscillation frequencies.

For the negative ion mode, the oscillation change was similar to that of the A/P-D curve measurement of the mouse brain sections. The oscillation phase (Fig. S6c) and amplitude (Fig. S6d) remained almost unchanged before the probe tapped the quartz. After the probe tapped the quartz (distance  $< 0$ ), the oscillation phase increased because of the repulsive interaction between the tip and quartz. The oscillation amplitude also decreased, and a nonlinear decrease region was observed when the probe oscillated at a higher frequency.



Table S1 Parameter settings for the laser puller.

	<b>HEAT</b>	<b>FIL</b>	<b>VEL</b>	<b>DEL</b>	<b>PUL</b>
<b>Line 1-7</b>	225	0	11	255	0

HEAT is the output power of the laser and the amount of energy supplied to the glass. VEL (velocity) specifies the velocity of the puller bar that moves before executing the hard pull for the capillary. DEL (delay) controls the timing of the start of the hard pull relative to the deactivation of the laser.